Zeolite Synthesis, Characterization and biological application of Zeolitic Nanoparticles

S. A. Gomkale¹, Dr. Manjusha Ugale², Dr. P. T. Kosankar³

¹Applied Chemistry, YCCE, Nagpur, India, shrutigomkale79@gmail.com
²Applied Chemistry, G.H.Raisoni, Nagpur, India, manjusha_g2@rediffmail.com
³Retired Applied Chemistry, YCCE, Nagpur, India, ptkosankar@gmail.com

Through chemical synthesis, zeolitic nanoparticles, offers a potential substitute for producing highvalue products. In order to create sodium aluminosilicate solutions with Si contents ranging from 1 to 8 molar, fumed silica and sodium aluminate were utilised. In this study, a single-phase zeolite A with high crystallinity was effectively produced using the alkali fusion hydrothermal technique. To identify as synthesised zeolites, X-ray diffraction (XRD), scanning electron microscopy (SEM), transmission electron microscope (TEM), and Fourier transform infrared (FT-IR) spectroscopy were used. The type and purity of zeolite were found to be strongly correlated with the synthesis circumstances and parameters, according to the results. The phases of the synthesised zeolites were identical, according to XRD results, and the 2 values were 19.76, 20.40, 20.86, 24.32, 26.34, 26.65, 27.00, 28.29, 35.51, and 39.29. The size of the crystallites was observed to vary between 1 µm. The internal Si-O-(Si) and Si-O-(Al) vibrations were found in the tetrahedra of aluminium and silicooxygen bridge in the range of 1200-400 cm-1, zeolite water in the range of 1600-3700 cm-1 and pseudo-lattice vibrations of structural unit in the range of 500-700 cm-1, according to the FTIR spectra. Inspecting the surface morphology of the powdered synthetic zeolite using SEM photomicrographs, it was discovered that it possessed a lamellar structure with a cubic edge and a crystal size. The width and length of the pores, which could be seen in TEM photomicrographs, were calculated to be 19.57 nm and 32.44 nm, respectively (length). The range of UV analysis was discovered to be 280 nm. Five different organisms were used to test the biological application.

Keywords: Zeolite, Synthesis, XRD, SEM, TEM, UV, FTIR, Biological application.

1. Introduction

Prosperity in the economy and in human life during the past few decades has necessitated massive energy use (Mandal and Sengupta, 2003). The majority of the world's energy is produced by fossil fuels and other renewable energy sources like sun, wind, hydropower and biomass. Zeolites are significant porous substances having open, organised three dimensional skeletons. Zeolites have been widely used in a number of industrial fields due to their huge specific surface area, superior cationic exchange capacity, heat stability, shape selection

selectivity, and other features (Mousavi et al., 2013; Hasan et al., 2012). Different zeolites, including X (Gomez et al., 2018), Y (Mastropietro et al., 2014), ZSM-5 (Kwan et al., 2010), MOR (Wang et al., 2018), and even pure silicon zeolite, have been successfully synthesised based on varied applications. In addition, zeolites have been altered and doped with the metals for a few particular processes. By doping silicalite-1 with vanadium or manganese, Zhao et al. (2018) successfully catalysed the selective oxidation of styrene on the material.

By interconnecting oxygen atoms in tetrahedral alumina (AlO45-) and silica (SiO44-), zeolites are hydrated aluminosilicates (Odebunmi et al., 2018; Omisanya et al., 2012). According to El Gaidoumi et al. (2011), the Greek terms "Zeo" and "Lithos," which translate to boil and stone, respectively, are the origin of the word "zeolite." Zeolites have a great capacity to absorb water and release it when heated (Moshoeshoe et al., 2017). Their 3D crystal structure coordinates active metals with aluminium, silicon, and oxygen in an open vacuum (Orjioke et al., 2016). Center atoms (Al, Si or P) and a terminal oxygen atom in a tetrahedral shape make up the basic components of zeolites. By forming rings, prisms, and other shapes by connecting oxygenoxygen atoms, zeolites can also produce secondary building blocks.

Tetrahedral SiO_4 and AlO_4 units make up the microporous, crystalline, hydrated aluminosilicates known as zeolites (Jha and Singh, 2011). Their main structural feature is the two-tetrahedral sharing of each oxygen atom in the three-dimensional tetrahedral framework. In the framework, Al^{3+} ions take the place of some Si4+ ions. Due to the difference in valency between the $(AlO_4)_5$ and $(SiO_4)_4$ tetrahedra, this results in a net negative charge that is frequently observed on one of the oxygen anions coupled to an aluminium cation (Weckhuysen and Yu, 2015). The counter ions, which are frequently alkali or alkaline earth metals like Na+, K+, or Ca2+, balance the resulting negative sites as a result (Armbruster and Gunter, 2001).

Zeolites are unusual materials with a high capacity for sorption as well as ion-exchange, molecular-sieve, and catalytic properties because of their regular channel and chamber architecture. Due to these qualities, zeolites have drawn a lot of attention from researchers. Any of the numerous minerals that fall within the category of hydrated aluminosilicates have a strong possible for significant request in the fields such as eliminating unwanted properties like porosity, surface area, and chemical resistance are prioritised in industries, heavy metal ions from industrial effluent streams can be found there (Erdem et al., 2004), environmental rehabilitation (Misaelides, 2011; Ghasemi et al., 2018) and treatment of water (Moshoeshoe et al., 2017), components for construction, energy storage, solar cooling, soil construction and maintenance, soil amendment, and animal nutrition and health (Nakhli et al., 2017), both molecular sieves and catalysts (Bacakova et al., 2018), etc. Most naturally occurring zeolites are created by volcanic activity, whereas synthetic zeolites are created when a basic medium reacts with sodium silicate, sodium aluminate, or coal combustion by-products (Franus, 2012; Wdowin et al., 2014). Due to the recent increase in demand for specialised and rare minerals like zeolites, finding a low-cost and effective method for their synthesis is still a challenging topic.

2. Materials and Methods

Preparation of zeolite A Acid pre-treatment

10 g of sodium aluminosilicate were separately refluxed at 45-95 °C for 0.5-4 hours in 50-300 mL of HCl solution (1.5–25%) to remove Fe_2O_3 (500 rpm). Following the reaction, the powder was cleaned by centrifuging it until the pH of the washing solution reached about 7 (Gomez et al., 2018). The powder was then dried overnight to completion.

Preparation of zeolite A

In order to modify between 0.5, 2.0 and 5.0 g mass ratios of NaOH to fly ash of sodium aluminosilicate that had been acid-treated, 2.05 g of sodium aluminium oxide (NaAlO₂), and the necessary amount of sodium hydroxide were ground and thoroughly combined in a paste. The combined paste was calcined together for two hours at high temperatures (550–850 °C) in air. After cooling to room temperature, the resultant solid product was pulverised, each combined with 5-45 mL of water, and aged for 12 hours while being stirred. The solid-liquid mixture was then autoclave-sealed and stored at a separate temperature of 60 to 95 °C for 6 to 24 hours. The resultant material was collected, allowed to cool to ambient temperature, and then wash away until the pH level was between 7-8. The resulting particles was then dried at 100 °C overnight. ZFA was the name given to the finished product.

Cation exchange capacity (CEC) test

CEC remained assessed using the simple ion exchange method, in which the Na+ ions in the zeolite's three-dimensional structure are exchanged out for NH4+ ions from an ammonium-containing solution. The heterogenous mixture was made up of 50 mL of 1000 mg L-1 NH4+ solution and 50 mL of 0.5 g ZFA, which were vibrated at 25 °C for 24 hours. Using a UV spectrophotometer (HACH, DR 5000, America) and Nessler's reagent spectrophotometry, the concentration of NH4+ was determined (Zhu et al., 2007). The functional relationship between absorbance and NH4+ level in solution was found, according to Chinese standard HJ 535-2009. The value of CEC was then determined by subtracting the initial reactive concentration from the equilibrium reactive concentration. The experiments were run three times, and the mean value was used to reduce confusion.

Characterization

UV-Vis Analysis

A UV-Vis spectrophotometer was used to evaluate the optical characteristics of zeolite A. At various time intervals extending up to 24 hours after the synthetic material was added, measurements of the spectra between 350 nm and 500 nm were taken. The spectra were acquired after zeolite A had been synthesised for 24 hours.

FT-IR analysis

Using an FT-IR spectrometer, the chemical composition of the produced zeolite A nanoparticles was investigated. The mixtures were dried at 75 °C, and the produced zeolite A was measured using the KBr pellet method between 400 and 400 cm⁻¹.

SEM and TEM Analysis

With the use of a scanning electron microscope and a transmission electron microscope, the

Nanotechnology Perceptions Vol. 20 No. S6 (2024)

morphological characteristics of a synthetic zeolite sample were examined (TEM). The SEM slides were made by smearing the solutions over slides after the zeolite had been produced for 24 hours. To make the samples conductors, a thin layer of platinum was applied to them. The samples were then investigated in the SEM with an accelerating voltage of 20 KV after that. XRD Analysis:

The chemical composition of kaolin was identified using a Rh X-ray tube and a Bruker S4 wavelength X-ray dispersive fluorescence spectrometer (WDXRFS). Phase characterisation was carried out using a Bruker AXS D4 ENDEAVOR diffractometer with Ni-filtered Cu Ka radiation at 40 kV and 40 mA. The measurements were made at 2 hours with a step width of 0.03 and a scan rate of 1 s per step. The diffraction data were examined using the Rietveld method utilising the DIFFRAC plus TOPAS software.

3. Results and Discussion

Natural zeolite contains unwanted components like metal oxides in addition to negative charge compensators like alkali and alkaline earth cations. The heterogeneous catalysts are enclosed in the structure when zeolite is produced naturally. The presence of such oxide pollutants may result in smaller pore diameters, which would reduce the effectiveness of zeolite matrices as adsorbents. These impurities would be eliminated from the zeolite matrix by activation.

Zeolite is crucial for industry, so researchers are working hard to figure out how it develops from its precursors. The technique of zeolite synthesis has drawn interest from scientists since it is possible to engineer the process to create a customised synthesised zeolite. It is essential for zeolite production to mimic natural geological processes. However, it is impossible because the development of zeolite took millions of years, whereas zeolite must be synthesised for commercial purposes in a matter of hours or days. To produce the desired zeolite with the desired qualities faster, the scientist must duplicate the optimal zeolite synthesis conditions. The hydrothermal process employed by scientists to create zeolite is one of the most unique techniques they employ. The lower production costs and ease of access are the key causes of this.

UV and FTIR Analysis

UV-vis analysis describes reflectance or absorption spectroscopy in the ultraviolet-visible spectrum. This implies that it makes use of nearby and visible light. The way the colours are seen is directly influenced by the substances' optical absorption or reflectance. Molecules go through electronic transitions in this area of the electromagnetic spectrum. The fundamental tenet of this theory is that molecules having n- or -electrons, which are unable to form bonds, can absorb energy from ultraviolet or visible light to excite these electrons to higher antibonding molecular orbitals. The longer the wavelength of light it can absorb, the easier it is for electrons to become excited (i.e., the lesser the energy gap between the HOMO and the LUMO). The zeolite-created nanoparticles' maximum absorbance was noted at about 280 nm and was shown as a peak on the spectrum.

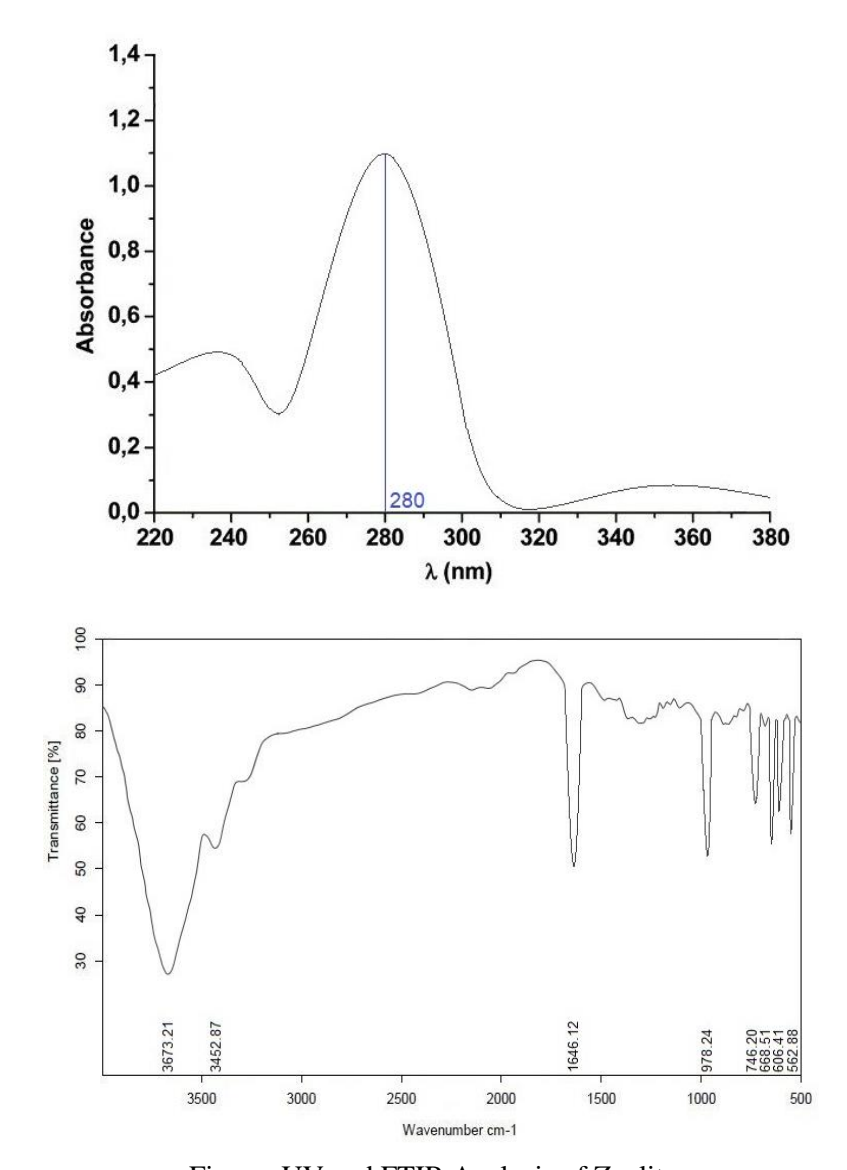


Figure: UV and FTIR Analysis of Zeolite

The measurement of IR radiation absorption by a sample plotted against wavelength is known as FT-IR spectroscopy. The correlation of the absorption bands (vibrational bands) with the chemical constituents in the sample is necessary for the interpretation of the IR spectra (Poovizhi and Krishnaveni, 2015). To determine the potential biomolecules in charge of the ion reduction and capping of the produced bio-reduced zeolite NPs, FTIR measurements are made.

The 1646 cm⁻¹ band of metakaolin, which has a zeolite structure, might be qualified to the antisymmetric stretching of T-O bonds (where T = Si or Al). When metakaolin and NaOH react, SiO_2 and Al_2O_3 are converted into aluminosilicates. A single band at roughly 1000 cm⁻¹, which is typical of Si-O-Al bonds in TO_4 tetrahedra, replaces their IR spectral vibration

Nanotechnology Perceptions Vol. 20 No. S6 (2024)

bands (Nesse, 2000). A wide band of poor intensity is visible around 562 cm⁻¹. This peak indicates the existence of the cubic prism-producing zeolite A band. The band at 553 cm⁻¹ may represent the beginning of the crystallisation of the double-ringed zeolite (Alkan et al., 2005). In the spectral region of 650-745 cm⁻¹, two unique peaks have been attributed to symmetric T-O-T vibrations of the sodalite framework, which are in good accord with the peaks of 668 and 606 cm⁻¹ for hydroxysodalite zeolite described by Flaningen et al., 1971.

There is a considerable assignment in the range of 1003- 970 cm⁻¹ with the literature for the unique bands between 1250 and 950 cm⁻¹ asymmetric stretching vibration for all zeolitic materials (Flaningen et al., 1971). A band at 3673 cm⁻¹ and a broad band at roughly 3452 cm⁻¹ are caused by zeolitic water. Thus, the results of the IR spectral research support the XRD findings. The reference IR wave numbers were specified as 1003, 662, 553, and 462 cm⁻¹ (Markovic et al., 2003). The IR spectra of a zeolite A sample are shown in Figure.

Scanning electron microscopy (SEM) and Transmission electron microscopy (TEM)

SEMs are used to examine solid surfaces and provide a variety of signals that reveal information about their morphology and topology (Nyankson et al., 2018). Chunfeng et al. 2019 used SEM to examine and contrast the structure of zeolites A and X. They noticed that zeolite X has an octahedral structure while zeolite A was created in the configuration of chamfered-edged cubes (Wang et al., 2012). Magdalena, 2001 used SEM to compare the one-step and multistep synthesis approaches in order to characterise the growth rate of zeolite.

The authors concluded that zeolites produced in several steps exhibit sharper shape than similar zeolites generated in a single step. They also realised that multistep visuals are more competent than single-step pictures. The authors failed to account for particle aggregation and the diffusion limit during characterisation.

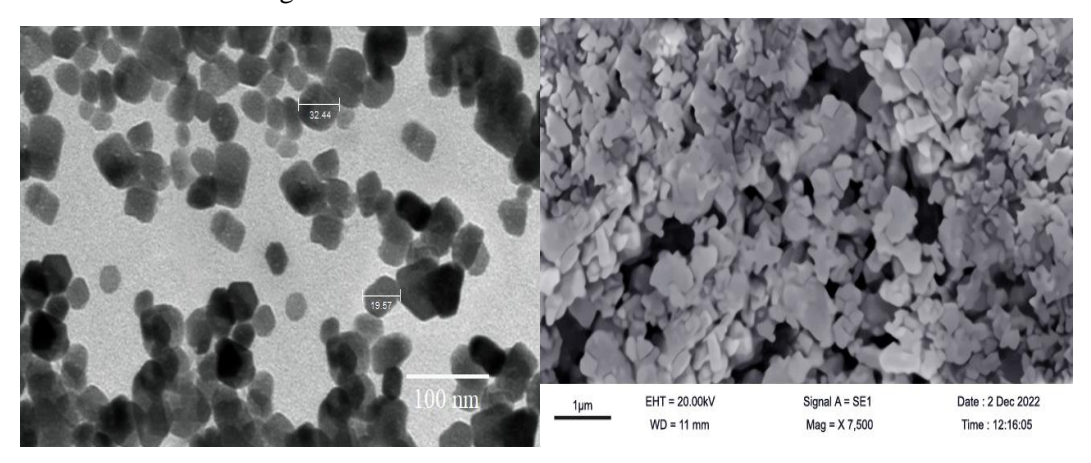


Figure: SEM and TEM Analysis of Synthesized Zeolite

The steady segments eventually attain the balance environments required to promote the crystal development of the finished zeolite materials (Fernandez-Jimenez et al., 2005). Zeolitization eventually produces the zeolite originators, which are composed of randomly ordered tetrahedrons of "Si" and "Al." These tetrahedrons are distributed uniformly along the cross-linked polymeric chains to create cavities that are suitable for receiving the Na ions that

balance charge. In conclusion, as porous materials, Na-zeolite crystals start to form and grow to a threshold point. The assimilation of particles from the solution through a growth process is known as crystallisation (Juan et al., 2007). Precipitating an aluminosilicate gel on the top of fly ash residues is another way to get aluminates and silicates to condense (Jansen, 1991). The inactive -quartz and inert mullite crystallites chemically react with NaOH to produce active forms of silicates (mainly) and aluminates, as shown by the following empirical formulas (scarcely).

 $SiO2(s) + 2NaOH(s) \rightarrow Na2SiO3(s) + H2O$

 $A12O3(s) + 2NaOH(s) \rightarrow 2NaAlO2(s) + H2O$

 $nNa2SiO3(s) + nNaAlO2(s) + yH2O \rightarrow Na2O.Al2O3.xSiO2.yH2O$

Here, "n" might be a complete number before a fraction. In contrast, "x," which ranges from two to ten but is primarily two, and "y," which represents the water molecules that fill the Nazeolite gaps, vary from two to seven (Baerlocher et al., 2007). Al_2O_3 and SiO_2 create the cationic framework because they combine oxygen atoms to create a tetrahedral crystalline structure (Mumpton et al., 1985).

XRD Analysis

RFA is primarily made up of mineral deposits of Al and Si in varying quantities of alumina and silica, according to the XRD patterns, which is further supported by data from XRF analysis. The phases of the produced zeolites were found to be comparable by XRD data and the 2θ values found to be 19.76, 20.40, 20.86, 24.32, 26.34, 26.65, 27.00, 28.29, 35.51 and 39.29. Peaks from the crystal phases of alumina (A), quartz (Q), NaX (X), NaZ (Z), NaP1 (P), and hydroxyl sodalite can be found in the synthesised products (S).

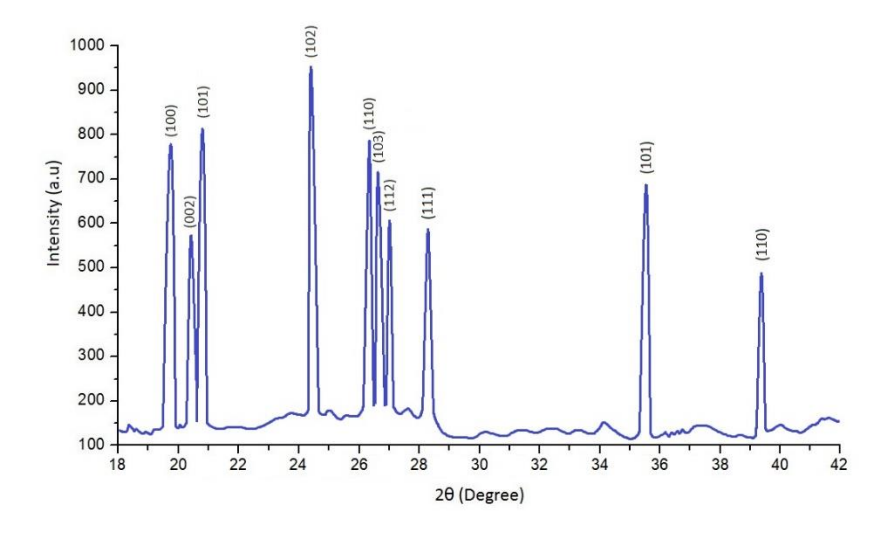


Figure: XRD Analysis of Synthesized Zeolite

It is evident that crystalline phases of Na-zeolites are generated by alkaline fusion with NaOH, as opposed to RFA, which failed to exhibit any peaks of aluminates or silicates. It was

Nanotechnology Perceptions Vol. 20 No. S6 (2024)

determined that the single-mode fusion method was inferior to fusion-assisted hydrothermal treatment because it revealed unreacted glassy phases such quartz (Q) and alumina together with NaX (X) and SOD (S) (A). High yields of high-grade zeolite product may be obtained by making wise choices for pH, temperature, reaction duration, and synthesis technique (Kokotailo and Fyfe, 1995). The existence of stable forms of silica including mullite and quartz, nonreactive hematite and magnetite phases and high concentrations of amorphous SiO₂ are observed to provide the maximum Na-zeolite yield, however the percentage yield drops as a result (Querol et al., 2001). These silica and alumina minerals in raw materials are what mostly convert sodium silicate (Na₂SiO₃) and sodium aluminosilicate (NaAlSiO₄) into Na-zeolites (Jha and Singh, 2016).

Antibacterial Activity

The results indicated that Synthesised Zeolite nanoparticles showed effective antibacterial activity against Gram -ve and Gram +ve. The antibacterial activity of Synthesised Zeolite nanoparticles was evaluated by measuring the zone of inhibition against E. coli, S.typhi, B. substilis, S.aureus and K.pneumoniae for different concentrations of the extract. The sizes of the zones of growth inhibition are presented in Table.

Table: Invitro Antibacterial activity of Synthesised Zeolite nanoparticles

Tuble: Invited Finite deterral detrity of Synthesised Zeonite nanoparticles					
Organisms	Control	Concentration (µl)			
	Control	20	30	40	50
Escherichia coli	20	12	15	18	21
Bacillus subtilis	23	11	15	19	22
Staphylococcus aureus	19	15	17	19	21
Salmonella typhi	21	10	13	17	19
Klebsiella pneumoniae	18	13	17	20	23

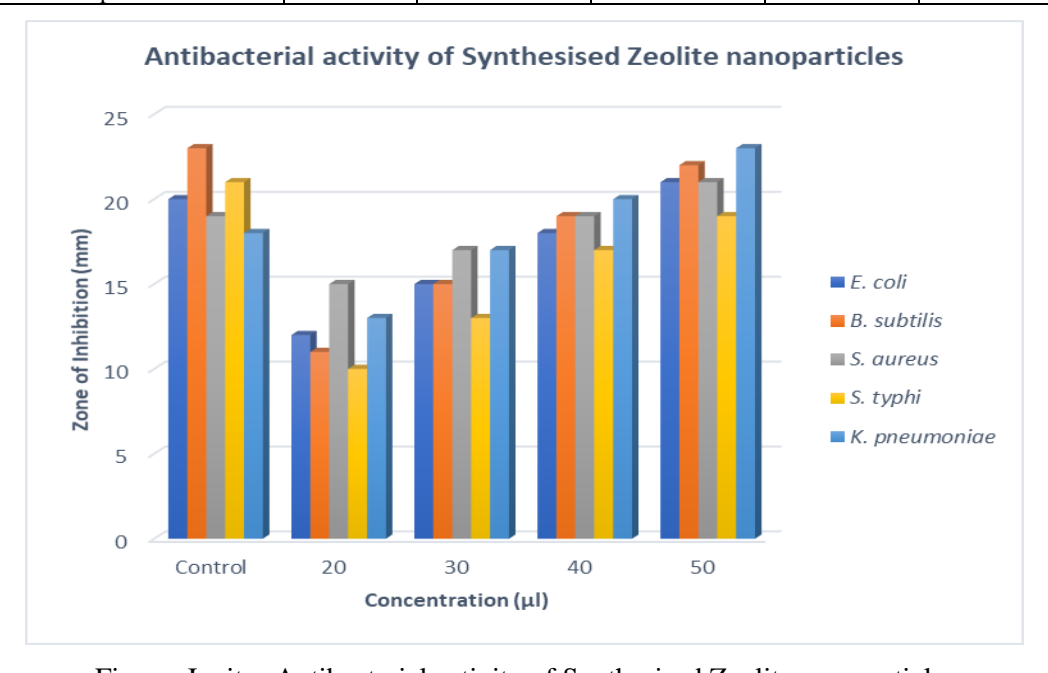


Figure: Invitro Antibacterial activity of Synthesised Zeolite nanoparticles

L. Magdalena, Synthesis, Characterization and Properties of Zeolite Films and Membranes, Lulea University of technology, Lule°

a, Sweden, 2001.

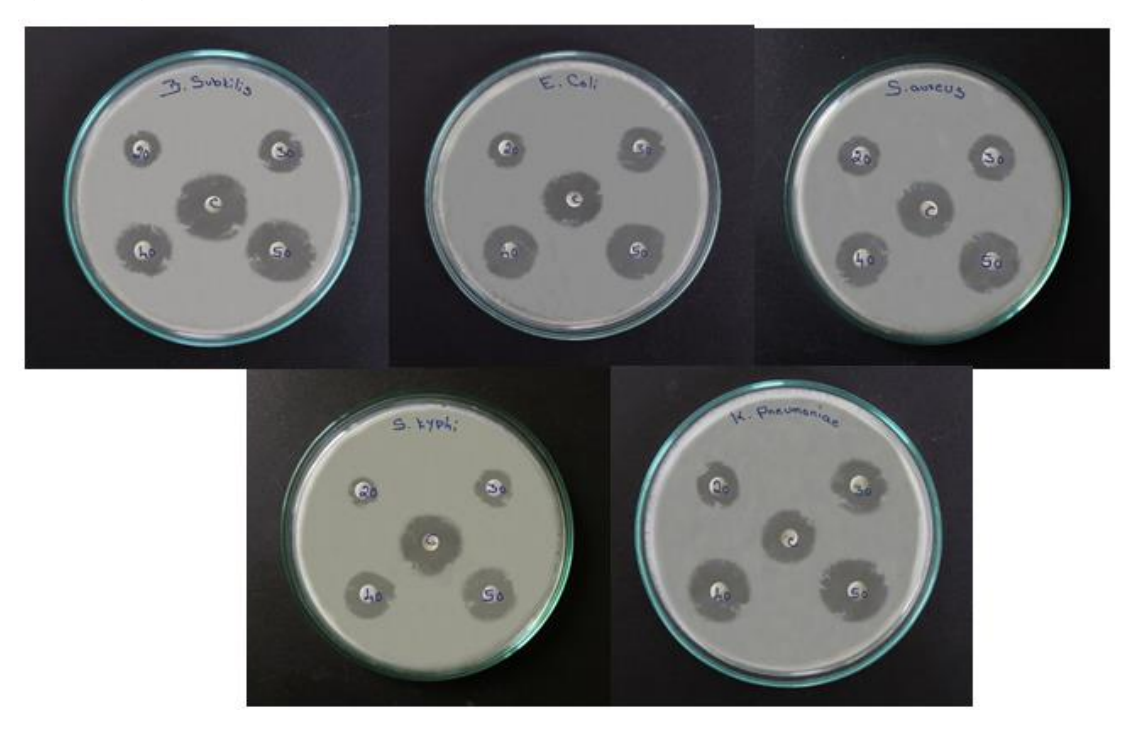


Figure: Invitro Antibacterial Activity

The findings demonstrated that all of the tested strains were effectively inhibited by synthesised zeolite nanoparticles. In general, the findings indicated that the concentration of Synthesized Zeolite nanoparticles increased the inhibitory impact. The outcomes for the biologically synthesised nanoparticles of zeolite were comparable to those attained for the control.

4. Conclusion

These are connected to their porosity and structural variety, consistent pore size and shape, mobility of cations, and hydrophilic and hydrophobic characteristics of the absorbents and absorbates, respectively. Due to zeolites' inherent qualities, they are used for a variety of purposes, such as water purification, membrane separation, coagulation, and antibacterial activities. Zeolites are still used in a variety of ways today to address issues related to the environment, science, and business. based on the zeolite formed by treating the activated metakaolin at 100°C for 20 hours' worth of XRD, IR, UV, TEM, and SEM findings. Based on the results of characterisation, zeolites display inherent traits such as homogenous pore size/shape, acidic properties, thermal stability, mobile cation, and surface properties such as *Nanotechnology Perceptions* Vol. 20 No. S6 (2024)

hydrophobicity and hydrophobicity. Along with catalysis, ion exchange, water filtration, adsorption, and agricultural uses, these are the principal applications for zeolite. The type of CFA used in the synthesis has no bearing on the zeolitization process. Additionally, the sample prepared for this experiment demonstrated strong sorption capacities when compared to commercially available natural and synthetic zeolites. Therefore, zeolites made with the suggested method could take their position as a less expensive substitute in technical applications that do not call for highly pure materials. The produced zeolite material's studied properties suggested that it might be effective as an adsorbent for several kinds of environmental contaminants.

References

- 1. Armbruster, T., & Gunter, M. E. (2001). Crystal structure of natural zeolites. Reviews in Mineralogy and Geochemistry, 45(1), 1–67. https://doi.org/10.2138/rmg.2001.45.1
- 2. Bacakova, L., Vandrovcova, M., Kopova, I., & Jirka, I. (2018). Applications of zeolites in biotechnology and medicine—A review. Biomaterials Science, 6(5), 974–989. https://doi.org/10.1039/C8BM00028J
- 3. Baerlocher, C., McCusker, L. B., & Olson, D. H. Atlas of zeolite framework types; Structure Commission of the International Zeolite Association. Elsevier. (2007).
- 4. El Gaidoumi, A., Benabdallah, A. C., Bali, B. E., & Kherbeche, A. (2011). Synthesis and characterization of zeolite HS using natural pyrophyllite as new clay source. Arabian Journal for Science and Engineering, 43, 1–8.
- 5. Erdem, E., Karapinar, N., & Donat, R. (2004). The removal of heavy metal cations by natural zeolites. Journal of Colloid and Interface Science, 280(2), 309–314. https://doi.org/10.1016/j.jcis.2004.08.028, PubMed: 15533402
- 6. Fernandez-Jiménez, A., Palomo, A., & Criado, M. (2005). Microstructure development of alkali- activated fly ash cement: A descriptive model. Cement and Concrete Research, 35(6), 1204–1209. https://doi.org/10.1016/j.cemconres.2004.08.021
- 7. Franus, W. (2012). Characterization of X-type zeolite prepared from coal fly ash. Polish Journal of Environmental Studies, 21, 337–343.
- 8. Ghasemi, Z., Sourinejad, I., Kazemian, H., & Rohani, S. (2018). Application of zeolites in aquaculture industry: A review. Reviews in Aquaculture, 10(1), 75–95. https://doi.org/10.1111/raq.12148
- 9. Gomez J. M., E. Díez, A. Rodríguez and M. Calvo, Microporous Mesoporous Mater., 2018, 270, 220—226.
- 10. Gómez, J. M., Díez, E., Rodríguez, A., & Calvo, M. (2018). Synthesis of mesoporous X zeolite using an anionic surfactant as templating agent for thermo-catalytic deoxygenation. Microporous and Mesoporous Materials, 270, 220–226. https://doi.org/10.1016/j.micromeso.2018.05.029
- 11. Hasan F., R. Singh, G. Li, D. Zhao and P. A. Webley, J. Colloid Interface Sci., 2012, 382, 1-12.
- 12. Jansen, J. C. (1991). The preparation of molecular sieves. In H. van Bekkum, E. M. Flanigen & J. C. Jansen (Eds.), Introduction to zeolite science and practice p. 754. Elsevier.
- 13. Jha, B., & Singh, D. N. (2011). A review on synthesis, characterization and industrial applications of fly ash zeolites. Journal of Materials Education, 33, 65–132.
- 14. Jha, B., & Singh, D. N. (2016). Advanced structured materials, fly ash zeolites innovations, applications and directions. Springer.
- 15. Juan, R., Hernández, S., Andrés, J. M., & Ruiz, C. (2007). Synthesis of granular zeolitic *Nanotechnology Perceptions* Vol. 20 No. S6 (2024)

- materials with high cation exchange capacity from agglomerated coal fly ash. Fuel, 86(12–13), 1811–1821. https://doi.org/10.1016/j.fuel.2007.01.011
- 16. Kokotailo, G. T., & Fyfe, C. A. (1995). Zeolite structure analysis with powder x-ray diffraction and solid-state NMR techniques. Rigaku J., 12, 3–10.
- 17. Kwan, S. M., Leung, A. Y. L., & Yeung, K. L. (2010). Gas permeation and separation in ZSM-5 micromembranes. Separation and Purification Technology, 73(1), 44–50. https://doi.org/10.1016/j.seppur.2009.10.015
- 18. Magdalena, L. (2001). Synthesis, characterization and properties of zeolite films and membranes. Lulea University of Technology°a. Sweden.
- 19. Mandal A. and D. Sengupta, Environ. Geol., 2003, 44, 180 —186.
- 20. Mastropietro, T. F., Drioli, E., & Poerio, T. (2014). Low temperature synthesis of nanosized NaY zeolite crystals from organic-free gel by using supported seeds. RSC Adv, 4(42), 21951–21957. https://doi.org/10.1039/C4RA03376K
- 21. Misaelides, P. (2011). Application of natural zeolites in environmental remediation: A short review. Microporous and Mesoporous Materials, 144(1–3), 15–18. https://doi.org/10.1016/j.micromeso.2011.03.024
- 22. Moshoeshoe, M., Nadiye-Tabbiruka, M. S., & Obuseng, V. (2017). A Review of the chemistry, structure, Properties and Applications of zeolites. American Journal of Materials Science, 7, 196–221.
- 23. Moshoeshoe, M., Nadiye-Tabbiruka, M. S., & Obuseng, V. (2017). A review of the chemistry, structure, properties and applications of zeolites. American Journal of Materials Science, 7, 196–221.
- 24. Mousavi S. F., M. Jafari, M. Kazemimoghadam and T. Mohammadi, Ceram. Int., 2013, 39, 7149 —7158.
- 25. Mumpton, F. A. (1985). Using zeolites in agriculture. In Innovative biological technologies for lesser developed countries. Proceedings, Office of Technology Assessment, US Congress: Washington, DC, United States; Workshop (pp. 125–158).
- 26. Nakhli, S. A. A., Delkash, M., Bakhshayesh, B. E., & Kazemian, H. (2017). Application of zeolites for sustainable agriculture: A review on water and nutrient retention. Water, Air, and Soil Pollution, 228(12), 464–498. https://doi.org/10.1007/s11270-017-3649-1
- 27. Nyankson, E., Efavi, J. K., Yaya, A., Manu, G., Asare, K., & Daafuor, J. (2018). Synthesis and characterization of zeolite-A and Zn-exchanged zeolite-A based on natural aluminosilicates and their potential applications. Cogent Engineering, 5, 1–23.
- 28. Odebunmi, E. O., Nwosu, F. O., Adeola, A. O., & Abayomi, T. G. Synthesis of zeolite from kaolin clay from ErusuAkoko southwestern Nigeria. G. Olaremu Journal of Chemical Society of Nigeria., 43, pp. 1–7. (2018).
- 29. Omisanya, N. O., Folayan, C. O., Aku, S. Y., & Adefila, S. S. (2012). Synthesis and characterization of zeolite a for adsorption refrigeration application. Advances in Applied Science Research, 6, 3746–3754.
- 30. Orjioke, M. N., Uchechukwu, O., Igwe, C. N., & Ajah, U. (2016). Synthesis and characterization of zeolite and its application in adsorption of nickel from aqueous solution. Journal Pharmaceutical and Chemical Biological Science, 4, 592–600.
- 31. Querol, X., Umaña, J. C., Plana, F., Alastuey, A., López-Soler, A., Medinaceli, A., Valero, A., Domingo, M. J., & Garcia-Rojo, E. G. (2001). Synthesis of zeolites from fly ash at pilot plant scale. Examples of potential applications. Fuel, 80(6), 857–865. https://doi.org/10.1016/S0016-2361(00)00156-3
- 32. Wang, C., Li, J., Sun, X., Wang, L., & Sun, X. (2009). Evaluation of zeolites synthesized from fly ash as potential adsorbents for wastewater containing heavy metals. Journal of Environmental Sciences, 21(1), 127–136. https://doi.org/10.1016/S1001-0742(09)60022-X
- 33. Wang, C., Shi, H., & Li, Y. (2012). Synthesis and characterization of natural zeolite supported

- Cr-doped TiO2 photocatalysts. Applied Surface Science, 258(10), 4328–4333. https://doi.org/10.1016/j.apsusc.2011.12.108
- 34. Wang, S. Y., He, B., Tian, R., Sun, C., Dai, R., Li, X., Wu, X., An, X., & Xie, X. (2018) Synthesis and catalytic performance of hierarchically structured MOR zeolites by a dual-functional templating approach. Journal of Colloid and Interface Science, 527, 339–345. https://doi.org/10.1016/j.jcis.2018.05.053
- Wdowin, M., Franus, M., Panek, R., Badura, L., & Franus, W. (2014). The conversion technology of fly ash into zeolites. Clean Technologies and Environmental Policy, 16(6), 1217–1223. https://doi.org/10.1007/s10098-014-0719-6
- 36. Weckhuysen, B. M., & Yu, J. (2015). Recent advances in zeolite chemistry and catalysis. Chemical Society Reviews, 44(20), 7022–7024. https://doi.org/10.1039/C5CS90100F
- 37. Zhao, J., Zhang, Y. F., Tian, F. P., Zuo, Y., Mu, Y., & Meng, C. G. (2018). High pH promoting the synthesis of V-Silicalite-1 with high vanadium content in the framework and its catalytic performance in selective oxidation of styrene. Dalton Transactions, 47(33), 11375–11385. https://doi.org/10.1039/c8dt02042f
- 38. Zhao, J., Zhang, Y. F., Zhang, S. Q., Wang, Q. S., Chen, M., Hu, T., & Meng, C. G. (2018). Synthesis and characterization of Mn-Silicalite-1 by the hydrothermal conversion of Mn-magadiite under the neutral condition and its catalytic performance on selective oxidation of styrene. Microporous and Mesoporous Materials, 268, 16–24. https://doi.org/10.1016/j.micromeso.2018.04.009
- 39. Zhu, L., Zhu, R., Xu, L., & Ruan, X. (2007). Influence of clay charge densities and surfactant loading amount on the microstructure of CTMA– montmorillonite hybrids. Colloids and Surfaces A: Physicochemical and Engineering Aspects, 304(1–3), 41–48. https://doi.org/10.1016/j.colsurfa.2007.04.019